

---

# Parallel Weight Consolidation: A Brain Segmentation Case Study

---

**Patrick McClure**

Section on Functional Imaging Methods  
National Institute of Mental Health  
patrick.mcclure@nih.gov

**Charles Y. Zheng**

Section on Functional Imaging Methods  
National Institute of Mental Health  
charles.zheng@nih.gov

**Francisco Pereira**

Section on Functional Imaging Methods  
National Institute of Mental Health  
francisco.pereira@nih.gov

**Jakub R. Kaczmarzyk**

McGovern Institute for Brain Research  
Massachusetts Institute of Technology  
jakubk@mit.edu

**John Rogers-Lee**

Section on Functional Imaging Methods  
National Institute of Mental Health  
john.rogers-lee@nih.gov

**Dylan Nielson**

Section on Functional Imaging Methods  
National Institute of Mental Health  
dylann.nielson@nih.gov

**Peter Bandettini**

Section on Functional Imaging Methods  
National Institute of Mental Health  
bandettini@nih.gov

## Abstract

Collecting the large datasets needed to train deep neural networks can be very difficult, particularly for the many applications for which sharing and pooling data is complicated by practical, ethical, or legal concerns. However, it may be the case that derivative datasets or predictive models developed within individual sites can be shared and combined with fewer restrictions. Training on distributed datasets and combining the resulting networks is often viewed as continual learning, but these methods require networks to be trained sequentially. In this paper, we introduce parallel weight consolidation (PWC), a continual learning method to consolidate the weights of neural networks trained in parallel on independent datasets. We perform a brain segmentation case study using PWC to consolidate several dilated convolutional neural networks trained in parallel on independent structural magnetic resonance imaging (sMRI) datasets from different sites. We found that PWC led to increased performance on held-out test sets from the different sites, as well as on a very large and completely independent multi-site dataset. This demonstrates the feasibility of PWC for combining the knowledge learned by networks trained on different datasets.

## 1 Introduction

Deep learning methods require large datasets to perform well. Collecting such datasets can be very difficult, particularly for the many applications for which sharing and pooling data is complicated by practical, ethical, or legal concerns. One prominent example are datasets collected on human

Layer	Filter	Padding	Dilation ( $l$ )	Non-linearity
1	$96 \times 3^3$	1	1	ReLU
2	$96 \times 3^3$	1	1	ReLU
3	$96 \times 3^3$	1	1	ReLU
4	$96 \times 3^3$	2	2	ReLU
5	$96 \times 3^3$	4	4	ReLU
6	$96 \times 3^3$	8	8	ReLU
7	$96 \times 3^3$	1	1	ReLU
8	$50 \times 1^3$	0	1	Softmax

Table 1: The Meshnet-like dilated convolutional neural network architecture used for brain segmentation.

participants, for which subjects sign informed consent agreements. These agreements can significantly limit the purposes for which the collected data can be used, even within a particular collection site. If the datasets are collected in a clinical setting, they may be subject to many additional constraints. However, it may be the case that derivative datasets or predictive models developed within individual sites can be shared and combined with fewer restrictions. Learning from non-centralized datasets is often viewed as continual learning, a sequential process where a given predictive model is updated to perform well on new datasets, while retaining the ability to predict on those previously used for training [27, 3, 19, 13]. The scenario we envisage is a more complex situation where multiple continual learning processes may take place in parallel. For instance, a given organization produces a starting model, which different, independent sites will then use with their own data. The sites will then contribute back updated models, which the organization will use to improve the main model being shared, with the goal of continuing the sharing and consolidation cycle.

Our application is segmentation of structural magnetic resonance imaging (sMRI) volumes. These segmentations are often generated using the Freesurfer package [7], a process that can take close to a day for each subject. The computational resources for doing this at a scale of hundreds to thousands of subjects are beyond the capabilities of most sites. We use deep neural networks to predict the Freesurfer segmentation *directly* from the structural volumes, as done previously by other groups [23]. We train several of those networks – each using data from a different site – in parallel and consolidate their weights. We show that this results in a model with improved generalization performance in test data from these sites, as well as a very large, completely independent multi-site dataset.

## 2 Data and Methods

### 2.1 Datasets

We use several sMRI datasets collected at different sites. We train networks using 956 sMRI volumes collected by the Human Connectome Project (HCP) [25], 1,136 sMRI volumes collected by the Nathan Kline Institute (NKI) [20], and 183 sMRI volumes collected by the Buckner Laboratory [1]. In order to provide an independent estimate of how well a given network generalizes to any new site, we also test networks on a completely held-out dataset consisting of 2,529 sMRI volumes collected across several institutions by the ABIDE project [4].

### 2.2 Architecture

Several deep neural network architectures have been proposed for brain segmentation, such as U-net [22], QuickNAT [23], HighResNet [15] and MeshNet [6, 5]. We chose MeshNet because of its relatively simple structure, its lower memory usage, and its competitive performance.

MeshNet uses dilated convolutional layers [26] due to the 3D structural nature of sMRI data. The output of these discrete volumetric dilated convolutional layers can be expressed as:

$$(w_f *_l h)_{i,j,k} = \sum_{\tilde{i}=-a}^a \sum_{\tilde{j}=-b}^b \sum_{\tilde{k}=-c}^c w_{f \tilde{i}, \tilde{j}, \tilde{k}} h_{i-l\tilde{i}, j-l\tilde{j}, k-l\tilde{k}} \quad (1)$$

where  $h$  is the input to the layer,  $a$ ,  $b$ , and  $c$  are the bounds for the  $i$ ,  $j$ , and  $k$  axes of the filter with weights  $w_f$ ,  $(i, j, k)$  is the voxel where the convolution is computed. The dilation factor  $l$  allows the convolution kernel to operate on every  $l$ -th voxel, since adjacent voxels are expected to be highly correlated. The dilation factor, number of filters, and other details of the MeshNet-like architecture that we used for all experiments is shown in Table 1.

## 2.3 Bayesian Inference in Neural Networks

### 2.3.1 Maximum a Posteriori Estimate

When training a neural network, the weights of the network,  $w$  are learned by optimizing  $\arg\max_w p(w|\mathcal{D})$  where  $\mathcal{D} = \{(x_1, y_1), \dots, (x_N, y_N)\}$  and  $(x_n, y_n)$  is the  $n$ th input-output example, per maximum likelihood estimation (MLE). However, this often overfits, so a maximum a posteriori (MAP) estimate given a prior on the network weights,  $p(w)$ , is used by maximizing:

$$\mathcal{L}_{MAP}(w) = \sum_{n=1}^N \log p(y_n|x_n, w) - \log p(w) \quad (2)$$

### 2.3.2 Approximate Bayesian Inference

In Bayesian inference for neural networks, a distribution of possible weights is learned instead of just a MAP point estimate. Using Bayes' rule,  $p(w|\mathcal{D}) = p(\mathcal{D}|w)p(w)/p(\mathcal{D})$  where  $p(w)$  is the prior over weights. However, directly computing the posterior,  $p(w|\mathcal{D})$ , is often intractable, particularly for DNNs. As a result, an approximate inference method must be used.

One of the most popular approximate inference methods for neural networks is variational inference, since it scales well to large DNNs. In variational inference, the posterior distribution  $p(w|\mathcal{D})$  is approximated by a learned variational distribution of weights  $q_\theta(w)$ , with parameters  $\theta$ . This approximation is enforced by minimizing the Kullback-Leibler divergence (KLD) between  $q_\theta(w)$ , and the true posterior,  $p(w|\mathcal{D})$ ,  $D_{KL}[q_\theta(w)||p(w|\mathcal{D})]$ . This is equivalent to maximizing the variational lower bound, also known as the evidence lower bound (ELBO) [8, 2, 11, 18, 17, 16]:

$$\mathcal{L}_{ELBO}(\theta) = \mathcal{L}_{\mathcal{D}}(\theta) - \mathcal{L}_{KLD}(\theta) \quad (3)$$

where  $\mathcal{L}_{\mathcal{D}}(\theta)$  is:

$$\mathcal{L}_{\mathcal{D}}(\theta) = \sum_{n=1}^N \mathbb{E}_{q_\theta(w)} [\log p(y_n|x_n, w)] \quad (4)$$

and  $\mathcal{L}_{KLD}(\theta)$  is the KLD between the variational distribution of weights and the prior.

$$\mathcal{L}_{KLD}(\theta) = D_{KL}[q_\theta(w)||p(w)] \quad (5)$$

Maximizing  $\mathcal{L}_{\mathcal{D}}$  seeks to learn a  $q_\theta(w)$  that explains the training data, while minimizing  $\mathcal{L}_{KLD}$  (i.e. keeping  $q_\theta(w)$  close to  $p(w)$ ) prevents learning a  $q_\theta(w)$  that overfits to the training data.

### 2.3.3 Stochastic Variational Bayes

Optimizing Eq. 3 for deep neural networks is usually impractical to compute, due to both: (1) being a full-batch approach and (2) integrating over  $q_\theta(w)$ . (1) is often dealt with by using stochastic mini-batch optimization [21] and (2) is often approximated using Monte Carlo sampling. [11] applied these methods to variational inference in deep neural networks. They used the "reparameterization trick" [12], which formulates  $q_\theta(w)$  as a deterministic differentiable function  $w = f(\theta, \epsilon)$  where  $\epsilon \sim \mathcal{N}(0, I)$ , to calculate an unbiased estimate of  $\nabla_\theta \mathcal{L}_{\mathcal{D}}$  for a mini-batch,  $\{(x_1, y_1), \dots, (x_M, y_M)\}$ , and one weight noise sample,  $\epsilon_m$ , for each mini-batch example:

$$\mathcal{L}_{ELBO}(\theta) \approx \mathcal{L}_{\mathcal{D}}^{SGVB}(\theta) - \mathcal{L}_{KLD}(\theta) \quad (6)$$

$$\mathcal{L}_{\mathcal{D}}(\theta) \approx \mathcal{L}_{\mathcal{D}}^{SGVB}(\theta) = \frac{N}{M} \sum_{m=1}^M \log p(y_m | x_m, f(\theta, \epsilon_m)) \quad (7)$$

### 2.3.4 Variational Continual Learning

In Bayesian neural networks,  $p(w)$  is often set to a multivariate Gaussian with diagonal covariance  $\mathcal{N}(\mathbf{0}, \sigma_{prior}^2 I)$ . (A variational distribution of the same form is called a fully factorized Gaussian (FFG).) However, instead of using a naïve prior, the parameters of a previously trained DNN can be used. Several methods, such as elastic weight consolidation [13] and synaptic intelligence [27], have explored this approach. Recently, these methods have been reinterpreted from a Bayesian perspective [19, 14]. In variational continual learning (VCL) [19] and Bayesian incremental learning [14], the DNNs trained on previously obtained data,  $D_1$ - $D_{T-1}$ , are used to regularize the training of a new neural network trained on  $D_T$  per:

$$p(w|D_{1:T}) = \frac{p(D_{1:T}|w)p(w)}{p(D_{1:T})} = \frac{p(D_{1:T-1}|w)p(D_T|w)p(w)}{p(D_{1:T-1})p(D_T)} = \frac{p(w|D_{1:T-1})p(D_T|w)}{p(D_T)} \quad (8)$$

where  $p(w|D_{1:T-1})$  is the network resulting from training on a sequence of datasets  $D_1$ - $D_{T-1}$ .

For DNNs, computing  $p(w|D_{1:T})$  directly can be intractable, so variational inference is iteratively used to learn an approximation,  $q_{\theta}^T(w)$ , by minimizing  $KLD[q_{\theta}^T(w)||p(w|D_{1:T})]$  for each sequential dataset,  $D_1$ - $D_T$ , in turn.

However, in many cases it is not feasible for one site to wait for another site to complete training, which can take days, in order to begin their own training. We seek to develop a method that will enable multiple sites to train their own networks in parallel and then bring the knowledge learned by each of these networks together in a new model.

## 2.4 Parallel Weight Consolidation

We propose parallel weight consolidation (PWC). This method takes neural networks which were independently trained in parallel on different datasets and consolidates their weights into one network.

### 2.4.1 Bayesian Parallel Learning

In PWC, we seek to consolidate several deep neural networks trained in parallel on  $S$  separate datasets,  $D_T = \{D_T^1, \dots, D_T^S\}$ , so that the resulting DNN can then be used to inform the training of a DNN on  $D_{T+1}$ . The training on each dataset starts from an existing network  $p(w|D_{1:T-1})$ .

Assuming that the  $S$  datasets are independent allows Eq. 8 to be rewritten as:

$$p(w|D_{1:T}) = \frac{p(w|D_{1:T-1}) \prod_{s=1}^S p(D_T^s|w)}{\prod_{s=1}^S p(D_T^s)} \quad (9)$$

However, training one of the  $S$  networks using VCL produces an approximation for  $p(w|D_{1:T-1}, D_T^s)$ . Eq. 9 can be written in terms of the learned distributions, since  $p(w|D_{1:T-1}, D_T^s) = p(w|D_{1:T-1})p(D_T^s|w)/p(D_T^s)$  per Eq. 8:

$$p(w|D_{1:T}) = \frac{1}{p(w|D_{1:T-1})^{S-1}} \prod_{s=1}^S p(w|D_{1:T-1}, D_T^s) \quad (10)$$

$p(w|D_{1:T-1})$  and each  $p(w|D_{1:T-1}, D_T^s)$  can be learned and then used to compute  $p(w|D_{1:T})$ . This distribution can then be used to learn  $p(w|D_{1:T+1})$  per Eq. 8.

### 2.4.2 Variational Approximation

In DNNs, however, directly calculating these probability distributions can be intractable, so variational inference is used to learn an approximation,  $q_\theta^{T,s}(w)$ , for  $p(w|D_{1:T-1}, D_T^s)$  by minimizing  $KLD[q_\theta^T(w)||p(w|D_{1:T-1}, D_T^s)]$ . This results in approximating Eq. 10 using:

$$p(w|D_{1:T}) \approx \frac{1}{q_\theta^{T-1}(w)^{S-1}} \prod_{s=1}^S q_\theta^{T,s}(w) \quad (11)$$

### 2.4.3 Dilated Convolutions with Fully Factorized Gaussian Filters

Although more complicated variational families have recently been explored in DNNs, the relatively simple FFG variational distribution can do as well as, or better than, more complex methods for continual learning [14]. In this paper, we use dilated convolutions with FFG filters. This assumes each filter is independent (i.e.  $p(w) = \prod_f p(w_f)$ ), that each weight within a filter is also independent (i.e.  $p(w_f) = \prod_{\tilde{i}=-a}^a \prod_{\tilde{j}=-b}^b \prod_{\tilde{k}=-c}^c p(w_{f,\tilde{i},\tilde{j},\tilde{k}})$ ), and that each weight is Gaussian (i.e.  $w_{f,\tilde{i},\tilde{j},\tilde{k}} \sim \mathcal{N}(\mu_{f,\tilde{i},\tilde{j},\tilde{k}}, \sigma_{f,\tilde{i},\tilde{j},\tilde{k}}^2)$ ). However, as discussed in [11, 18], randomly sampling each weight for each mini-batch example can be computationally expensive, so the fact that the sum of independent Gaussian variables is also Gaussian is used to move the noise from the weights to the convolution operation. For, dilated convolutions, this is described by:

$$(w_f * h)_{i,j,k} \sim \mathcal{N}(\mu_{f,i,j,k}^*, (\sigma_{f,i,j,k}^*)^2) \quad (12)$$

$$\mu_{f,i,j,k}^* = \sum_{\tilde{i}=-a}^a \sum_{\tilde{j}=-b}^b \sum_{\tilde{k}=-c}^c \mu_{f,\tilde{i},\tilde{j},\tilde{k}} h_{i-l\tilde{i},j-l\tilde{j},k-l\tilde{k}} \quad (13)$$

$$(\sigma_{f,i,j,k}^*)^2 = \sum_{\tilde{i}=-a}^a \sum_{\tilde{j}=-b}^b \sum_{\tilde{k}=-c}^c \sigma_{f,\tilde{i},\tilde{j},\tilde{k}}^2 h_{i-l\tilde{i},j-l\tilde{j},k-l\tilde{k}}^2 \quad (14)$$

Eq. 12 can be rewritten using the Gaussian "reparameterization trick":

$$(w_f * h)_{i,j,k} = \mu_{f,i,j,k}^* + \sigma_{f,i,j,k}^* \epsilon_{f,i,j,k} \text{ where } \epsilon_{f,i,j,k} \sim \mathcal{N}(0, 1) \quad (15)$$

### 2.4.4 Consolidating an Ensemble of Fully Factorized Gaussian Networks

Eq. 11 can be used to consolidate an ensemble of parallelly trained networks in order to allow for training on new datasets. Eq. 11 can be directly calculated if  $q_\theta^{T-1}(w_{f,\tilde{i},\tilde{j},\tilde{k}}) = \mathcal{N}(\mu_{f,0,\tilde{i},\tilde{j},\tilde{k}}, \sigma_{f,0,\tilde{i},\tilde{j},\tilde{k}}^2)$  and  $q_\theta^{T,s}(w_{f,\tilde{i},\tilde{j},\tilde{k}}) = \mathcal{N}(\mu_{f,s,\tilde{i},\tilde{j},\tilde{k}}, \sigma_{f,s,\tilde{i},\tilde{j},\tilde{k}}^2)$  are known, resulting in  $p(w|D_{1:T})$  also being an FFG:

$$p(w_{f,\tilde{i},\tilde{j},\tilde{k}}|D_{1:T}) \propto \prod_{s=1}^{S-1} e^{\frac{(w_{f,0,\tilde{i},\tilde{j},\tilde{k}} - \mu_{f,0,\tilde{i},\tilde{j},\tilde{k}})^2}{2\sigma_{f,0,\tilde{i},\tilde{j},\tilde{k}}^2}} \prod_{s=1}^S e^{\frac{-(w_{f,s,\tilde{i},\tilde{j},\tilde{k}} - \mu_{f,s,\tilde{i},\tilde{j},\tilde{k}})^2}{2\sigma_{f,s,\tilde{i},\tilde{j},\tilde{k}}^2}} \quad (16)$$

$$p(w_{f,\tilde{i},\tilde{j},\tilde{k}}|D_{1:T}) \approx \mathcal{N}\left(\frac{\sum_{s=1}^S \frac{\mu_{f,s,\tilde{i},\tilde{j},\tilde{k}}}{\sigma_{f,s,\tilde{i},\tilde{j},\tilde{k}}^2} - \sum_{s=1}^{S-1} \frac{\mu_{f,0,\tilde{i},\tilde{j},\tilde{k}}}{\sigma_{f,0,\tilde{i},\tilde{j},\tilde{k}}^2}}{\sum_{s=1}^S \frac{1}{\sigma_{f,s,\tilde{i},\tilde{j},\tilde{k}}^2} - \sum_{s=1}^{S-1} \frac{1}{\sigma_{f,0,\tilde{i},\tilde{j},\tilde{k}}^2}}, \frac{1}{\sum_{s=1}^S \frac{1}{\sigma_{f,s,\tilde{i},\tilde{j},\tilde{k}}^2} - \sum_{s=1}^{S-1} \frac{1}{\sigma_{f,0,\tilde{i},\tilde{j},\tilde{k}}^2}}\right) \quad (17)$$

Eq. 17 follows from Eq. 16 by completing the square inside the exponent and matching the parameters to the multivariate Gaussian density; it is defined when  $\sum_{s=1}^S \frac{1}{\sigma_{f,s,\tilde{i},\tilde{j},\tilde{k}}^2} - \sum_{s=1}^{S-1} \frac{1}{\sigma_{f,0,\tilde{i},\tilde{j},\tilde{k}}^2} > 0$ . To ensure this, we constrained  $\sigma_{f,0,\tilde{i},\tilde{j},\tilde{k}}^2 \geq \sigma_{f,s,\tilde{i},\tilde{j},\tilde{k}}^2$ . This should be the case if the loss is optimized,

<i>Network</i>	<i>H</i>	<i>N</i>	<i>B</i>	<i>Avg.</i>	<i>A</i>
$H_{MAP}$	82.25	65.88	67.94	72.92	55.25
$N_{MAP}$	71.2	72.19	70.73	71.66	66.67
$B_{MAP}$	65.69	50.17	82.02	59.25	50.23
<i>Ensemble</i>	79.85	71.08	80.62	75.53	63.35
$H \rightarrow N$	75.40	73.24	71.77	74.03	64.62
$H \rightarrow B$	73.85	56.79	79.49	65.78	49.27
$H \rightarrow N + B$	70.25	71.5	72.13	71.03	59.04
$H \rightarrow N \rightarrow H$	82.23	70.65	73.14	75.72	61.92
$H \rightarrow B \rightarrow H$	82.77	69.14	77.79	75.56	59.88
$H \rightarrow N + B \rightarrow H$ (PWC)	81.35	74.72	78.30	77.79	67.56

Table 2: The average Dice scores across test volumes for the trained networks on HCP (H), NKI (N), and Buckner (B), along with the weighted average Dice scores across H, N, and B and the average Dice scores across volumes on the independent ABIDE (A) dataset.

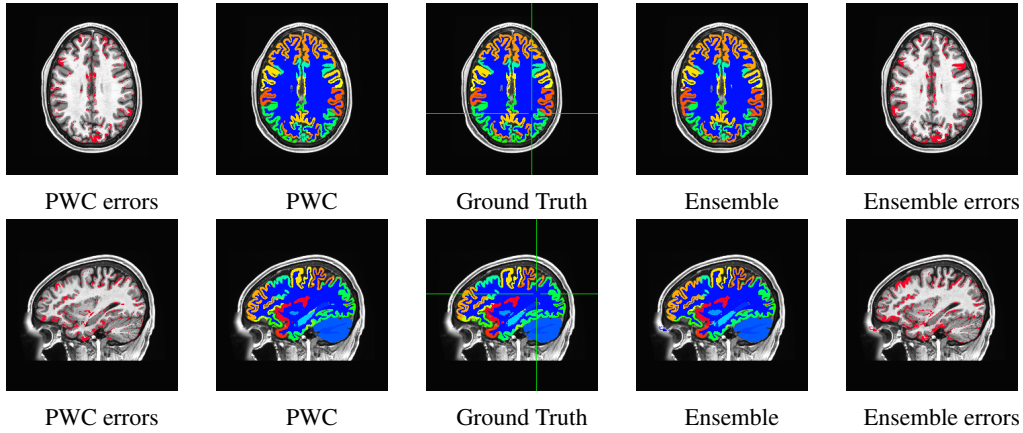


Figure 1: The axial and sagittal segmentations produced by PWC and the ensemble baseline on a HCP subject. The subject was selected by matching the subject specific Dice with the average Dice across HCP. Segmentations errors for all classes are shown in red in the respective plot.

since  $\mathcal{L}_{\mathcal{D}}$  should pull  $\sigma_{f,s,\tilde{i},\tilde{j},\tilde{k}}^2$  to 0 and  $\mathcal{L}_{KLD}$  pulls  $\sigma_{f,s,\tilde{i},\tilde{j},\tilde{k}}^2$  towards  $\sigma_{f,0,\tilde{i},\tilde{j},\tilde{k}}^2$ .  $p(w_{f,\tilde{i},\tilde{j},\tilde{k}}|D_{1:T})$  can then be used as a prior for training another variational DNN.

### 3 Experiments

#### 3.1 Experimental Setup

##### 3.1.1 Data Preprocessing

All structural MRI datasets were collected with MPRAGE sequences, with a grid of  $128 \times 128 \times 128$   $2mm^3$  voxels. The data for each subject was aligned to the MNI-152 brain template with a rigid transformation [9]. This preserved the structure of each individual brain, while positioning them all on the same central position in the 3D volume. We computed 50-class Freesurfer [7] segmentations, as in [5], for all subjects in each of the datasets described earlier. These were used as the labels for prediction. A 90-10 training-test split was used for the HCP, NKI, and Buckner datasets. During training and testing, input volumes were individually z-scored across voxels. Similar to [6, 5], we split each input volume into 64  $32 \times 32 \times 32$  sub-volumes.

##### 3.1.2 Training Procedure

All networks were trained with Adam [10] and an initial learning rate of 0.001. The MAP networks were trained until convergence. The subsequent networks were trained until the training loss started

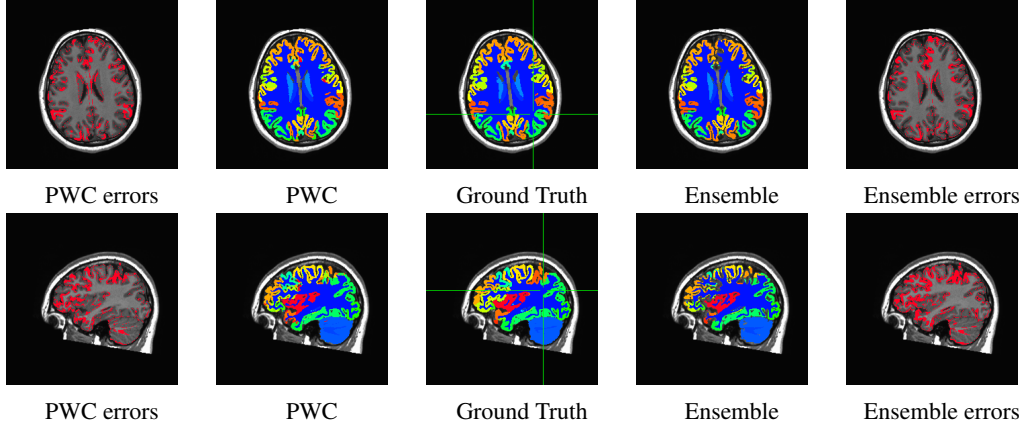


Figure 2: The axial and sagittal segmentations produced by PWC and the ensemble baseline on a NKI subject. The subject was selected by matching the subject specific Dice with the average Dice across NKI. Segmentations errors for all classes are shown in red in the respective plot.

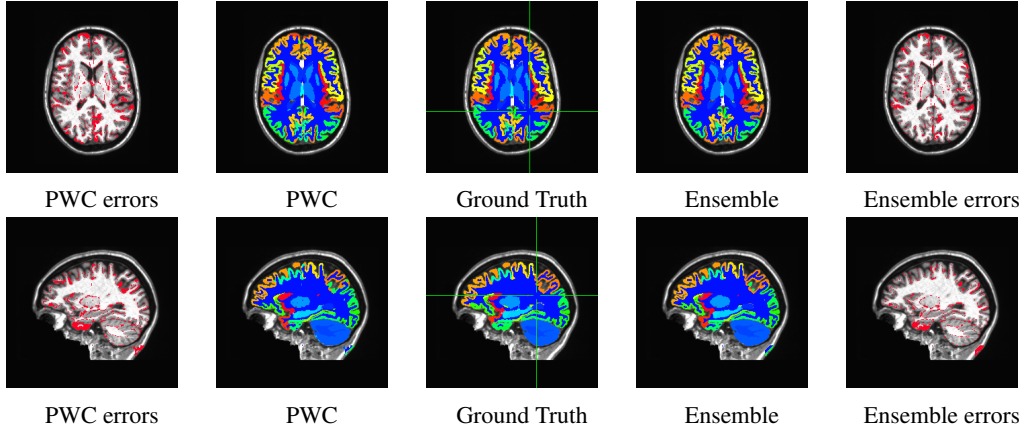


Figure 3: The axial and sagittal segmentations produced by PWC and the ensemble baseline on a Buckner subject. The subject was selected by matching the subject specific Dice with the average Dice across Buckner. Segmentations errors for all classes are shown in red in the respective plot.

to oscillate around a stable loss value. These networks trained much faster than the MAP networks, since they were initialized with previously trained networks. The batch-size was set to 10. Weight normalization [24] was used for the weight means for all networks and the weight standard deviations were initialized to 0.001 as in [16] for the variational network trained on HCP. For  $H_{MAP}$  and the variational network trained on HCP,  $p(w) = \mathcal{N}(0, 1)$ .

### 3.1.3 Performance Metric

To measure the quality of the produced segmentations, we calculated the Dice coefficient, which is defined by:

$$Dice_c = \frac{2|\hat{Y}_c \cap Y_c|}{|\hat{Y}_c| + |Y_c|} = \frac{2TP_c}{2TP_c + FN_c + FP_c} \quad (18)$$

where  $\hat{Y}_c$  is the binary segmentation for class  $c$  produced by a network,  $Y_c$  is the ground truth produced by Freesurfer,  $TP_c$  is the true positive rate for class  $c$ ,  $FN_c$  is the false negative rate for class  $c$ , and  $FP_c$  is the false positive rate for class  $c$ . We calculate the Dice coefficient for each class  $c$  and average across classes to compute the overall performance of a network.

### 3.2 Baselines

We trained MAP networks on the HCP ( $H_{MAP}$ ), the NKI ( $N_{MAP}$ ), and Buckner ( $B_{MAP}$ ) datasets. We averaged the output probabilities of the  $H_{MAP}$ ,  $N_{MAP}$ , and  $B_{MAP}$  to create an ensemble baseline. The Dice scores for these networks are shown in Table 2.

### 3.3 Parallel Weight Consolidation

For ensemble consolidation (EC) our goal was to take networks trained in parallel using VCL with an initial network as a prior, consolidate them per Eq. 17, and then use this consolidated model as a prior for training on the original dataset. To test this, we: (1) trained an initial FFG variational network on HCP (H) using  $H_{MAP}$  to initialize the network, (2) used VCL with H as the prior for parallelly training FFG variational networks on the NKI ( $H \rightarrow N$ ) and Buckner ( $H \rightarrow B$ ) datasets, (3) then used PWC to consolidate  $H \rightarrow N$  and  $H \rightarrow B$  into  $H \rightarrow N + B$  per Eq. 17, and (4) used  $H \rightarrow N + B$  as a prior for training an FFG variational network on  $H$  ( $H \rightarrow N + B \rightarrow H$ ). We compared  $H \rightarrow N + B \rightarrow H$  to: (1) transferring from HCP to NKI back to HCP using VCL ( $H \rightarrow N \rightarrow H$ ), (2) transferring from HCP to Buckner back to HCP using VCL ( $H \rightarrow B \rightarrow H$ ), and (3) an ensemble of MAP networks each trained on either the HCP ( $H_{MAP}$ ), NKI ( $N_{MAP}$ ), or Buckner ( $B_{MAP}$ ) data. For the variational networks, 10 MC samples were used during test time to approximate the expected network output. The average DICE scores across classes and sMRI volumes are shown in Table 2. In Figures 1, 2, and 3, we show selected example segmentations that have Dice scores similar to the average Dice score across the respective dataset. PWC led to both robustness to contrast differences between the datasets and robustness to input skew. Using PWC to consolidate the H, N, and B networks increases the weighted average Dice score, where the H, N, and B scores are weighted according to the number of volumes in each, and increases the Dice score for the completely independent, held-out ABIDE dataset.

## 4 Discussion

There are many problem for which accumulating data into one accessible dataset for training can be difficult or impossible, such as for clinical data. It may, however, be feasible to share models derived from such data. A method often proposed for dealing with these independent datasets is continual learning, which trains on each of these datasets sequentially [3]. Several recent continual learning methods use previously trained networks as priors for networks trained on the next dataset [27, 19, 13]. We developed PWC by modifying these methods to allow for training networks on several new datasets in parallel. Using PWC, we consolidated the weights of the neural networks that were trained in parallel to perform brain segmentation on data from different sites, to form a prior distribution for further training. We found that using this consolidated knowledge as a prior for training on the original site via PWC increased performance on both the test sets for the visited sites and ABIDE, compared to an ensemble made from models trained on different sites. This demonstrates the feasibility of PWC for combining the knowledge learned by networks trained on different datasets. One important direction for future research is scaling PWC up to allow for consolidating many more networks trained in parallel and repeating this training and consolidation cycle several times. Another area of research is to investigate the use of alternative families of variational distributions within the framework of PWC. Our method has the potential to be applied to many other applications where it is necessary to train specialized networks for specific sites, informed by data from other sites, and where constraints on data sharing necessitate a distributed learning approach, such as disease diagnosis with clinical data.

## References

- [1] Bharat B Biswal, Maarten Mennes, Xi-Nian Zuo, Suril Gohel, Clare Kelly, Steve M Smith, Christian F Beckmann, Jonathan S Adelstein, Randy L Buckner, Stan Colcombe, et al. Toward discovery science of human brain function. *Proceedings of the National Academy of Sciences*, 107(10):4734–4739, 2010.
- [2] Charles Blundell, Julien Cornebise, Koray Kavukcuoglu, and Daan Wierstra. Weight uncertainty in neural network. In *International Conference on Machine Learning*, pages 1613–1622, 2015.



- [3] Ken Chang, Niranjana Balachandrar, Carson Lam, Darwin Yi, James Brown, Andrew Beers, Bruce Rosen, Daniel L Rubin, and Jayashree Kalpathy-Cramer. Distributed deep learning networks among institutions for medical imaging. *Journal of the American Medical Informatics Association*.
- [4] Adriana Di Martino, Chao-Gan Yan, Qingyang Li, Erin Denio, Francisco X Castellanos, Kaat Alaerts, Jeffrey S Anderson, Michal Assaf, Susan Y Bookheimer, Mirella Dapretto, et al. The autism brain imaging data exchange: towards a large-scale evaluation of the intrinsic brain architecture in autism. *Molecular Psychiatry*, 19(6):659, 2014.
- [5] Alex Fedorov, Eswar Damaraju, Vince Calhoun, and Sergey Plis. Almost instant brain atlas segmentation for large-scale studies. *arXiv preprint arXiv:1711.00457*, 2017.
- [6] Alex Fedorov, Jeremy Johnson, Eswar Damaraju, Alexei Ozerin, Vince Calhoun, and Sergey Plis. End-to-end learning of brain tissue segmentation from imperfect labeling. In *International Joint Conference on Neural Networks*, pages 3785–3792. IEEE, 2017.
- [7] Bruce Fischl. Freesurfer. *Neuroimage*, 62(2), 2012.
- [8] Alex Graves. Practical variational inference for neural networks. In *Advances in Neural Information Processing Systems*, pages 2348–2356, 2011.
- [9] Mark Jenkinson, Christian F Beckmann, Timothy EJ Behrens, Mark W Woolrich, and Stephen M Smith. Fsl. *Neuroimage*, 62(2):782–790, 2012.
- [10] Diederik P Kingma and Jimmy Ba. Adam: A method for stochastic optimization. 2015.
- [11] Diederik P Kingma, Tim Salimans, and Max Welling. Variational dropout and the local reparameterization trick. In *Advances in Neural Information Processing Systems*, pages 2575–2583, 2015.
- [12] Diederik P Kingma and Max Welling. Auto-encoding variational bayes. *arXiv preprint arXiv:1312.6114*, 2013.
- [13] James Kirkpatrick, Razvan Pascanu, Neil Rabinowitz, Joel Veness, Guillaume Desjardins, Andrei A Rusu, Kieran Milan, John Quan, Tiago Ramalho, Agnieszka Grabska-Barwinska, et al. Overcoming catastrophic forgetting in neural networks. *Proceedings of the National Academy of Sciences*, 114(13):3521–3526, 2017.
- [14] Max Kochurov, Timur Garipov, Dmitry Podoprikin, Dmitry Molchanov, Arsenii Ashukha, and Dmitry Vetrov. Bayesian incremental learning for deep neural networks. *ICLR Workshop*, 2018.
- [15] Wenqi Li, Guotai Wang, Lucas Fidon, Sebastien Ourselin, M Jorge Cardoso, and Tom Vercauteren. On the compactness, efficiency, and representation of 3d convolutional networks: brain parcellation as a pretext task. In *International Conference on Information Processing in Medical Imaging*, pages 348–360. Springer, 2017.
- [16] Christos Louizos and Max Welling. Multiplicative normalizing flows for variational bayesian neural networks. In *International Conference on Machine Learning*, pages 2218–2227, 2017.
- [17] Patrick McClure and Nikolaus Kriegeskorte. Representing inferential uncertainty in deep neural networks through sampling. *NIPS Bayesian Deep Learning Workshop*, 2017.
- [18] Dmitry Molchanov, Arsenii Ashukha, and Dmitry Vetrov. Variational dropout sparsifies deep neural networks. In *International Conference on Machine Learning*, pages 2498–2507, 2017.
- [19] Cuong V Nguyen, Yingzhen Li, Thang D Bui, and Richard E Turner. Variational continual learning. 2018.
- [20] Kate Brody Nooner, Stanley Colcombe, Russell Tobe, Maarten Mennes, Melissa Benedict, Alexis Moreno, Laura Panek, Shaquanna Brown, Stephen Zavitz, Qingyang Li, et al. The nki-rockland sample: a model for accelerating the pace of discovery science in psychiatry. *Frontiers in Neuroscience*, 6:152, 2012.
- [21] Herbert Robbins and Sutton Monro. A stochastic approximation method. *The Annals of Mathematical Statistics*, pages 400–407, 1951.
- [22] Olaf Ronneberger, Philipp Fischer, and Thomas Brox. U-net: Convolutional networks for biomedical image segmentation. In *International Conference on Medical Image Computing and Computer-Assisted Intervention*, pages 234–241. Springer, 2015.
- [23] Abhijit Guha Roy, Sailesh Conjeti, Nassir Navab, and Christian Wachinger. Quicknat: Segmenting mri neuroanatomy in 20 seconds. *arXiv preprint arXiv:1801.04161*, 2018.

- [24] Tim Salimans and Diederik P Kingma. Weight normalization: A simple reparameterization to accelerate training of deep neural networks. In *Advances in Neural Information Processing Systems*, pages 901–909, 2016.
- [25] David C Van Essen, Stephen M Smith, Deanna M Barch, Timothy EJ Behrens, Essa Yacoub, Kamil Ugurbil, Wu-Minn HCP Consortium, et al. The wu-minn human connectome project: an overview. *NeuroImage*, 80:62–79, 2013.
- [26] Fisher Yu and Vladlen Koltun. Multi-scale context aggregation by dilated convolutions. *arXiv preprint arXiv:1511.07122*, 2015.
- [27] Friedemann Zenke, Ben Poole, and Surya Ganguli. Continual learning through synaptic intelligence. In *International Conference on Machine Learning*, pages 3987–3995, 2017.